Int. J. Heat Mass Transfer. Vol. 30, No. 7, pp. 1487–1495, 1987
Printed in Great Britain

0017–9310/87 $3.00 + 0.00

Effect of natural convection and thermal transparency of liquid encapsulant on thermal stresses during LEC growth of GaAs

SHAHRYAR MOTAKEF
Department of Mechanical Engineering, Massachusetts Institute of Technology, Cambridge, MA 02139, U.S.A.

(*Received* 26 *June* 1986 *and in final form* 6 *January* 1987)

Abstract—The effects of natural convection and thermal transparency of the liquid encapsulant on the temperature and elastic stress distributions in GaAs crystals grown by the low pressure liquid-encapsulated Czochralski (LP-LEC) technique are numerically investigated. The results indicate that the stresses exceed CRSS appreciably during conventional LP-LEC growth and can be significantly reduced by total encapsulation of the growing solid.

INTRODUCTION

RECENT advances in high performance GaAs IC technologies have resulted in increased demand for high quality, large diameter semi-insulating substrate material. Presently the materials requirements are considered to be: (a) low background impurity levels, (b) reproducibility and high resistivity with thermal stability, and (c) high degree of crystalline perfection [1]. Furthermore, the viable development of GaAs IC technology requires use of standard semiconductor processing equipment designed for large diameter round silicon wafers. The physical, chemical, and crystalline requirements imposed on GaAs materials have resulted in an intense effort in the application of liquid encapsulated Czochralski (LEC) technique to the growth of GaAs. The primary crystalline defect in LEC grown GaAs crystals is the high density of dislocations (10^4–10^5 cm^{-2}) which are associated with the large thermal stresses present in the crystal during growth. Although harmful effects of high dislocation densities on the performance of majority carrier devices such as MESFETs is not yet clearly established, their deleterious effect on the performance of minority carrier devices such as LEDs and laser structures appears to be well recognized [2]. It is generally accepted that significant reduction in the density of dislocations is required for improved performance of opto-electronic as well as digital and monolithic IC devices.

The principal cause of dislocations in bulk GaAs crystals is excessive thermal stresses experienced by the solid during growth. As the resolved shear stress exceeds a critical value, the so-called critical resolved shear stress (CRSS), glide along the crystallographic slip system and an associated generation of dislocations is initiated. Approaches to the reduction of the density of stress-related dislocations focus primarily on: (1) increasing the critical resolved shear stress of the system through lattice-hardening by iso-electronic doping and (2) reduction of thermal gradients in the solid. Problems associated with the thermal stability (during processing) and device performance of doped substrate materials as well as growth interface breakdown due to constitutional supercooling of the melt suggest approaches based on heat transfer control with use of iso-electronic doping at minimized concentration levels. Reduction of temperature gradients in the growing solid through increased thickness of liquid encapsulant [3] and the use of after-heaters or heat reflectors [4] have resulted in a noticeable reduction in the density of dislocations. Nevertheless, dislocation-free 75 mm (3 in) LEC grown GaAs crystals have not yet been produced.

The thermal stress distribution in GaAs crystals grown by the LEC technique was first obtained by Jordan *et al.* [5]. Whereas the plane-strain assumption in Jordan's model, similar to previous works by Penning [6], Advonin *et al.* [7], and Brice [8], have been shown to be invalid [9, 10], the major discrepancy between the experimental observations and Jordan *et al.*'s results can be traced to the heat transfer component of their study. Specifically, by using an average heat transfer coefficient in the encapsulant (from existing correlations for natural convection along vertical surfaces), and a constant environment temperature for both the encapsulated and exposed portion of the crystal they concluded that the density of thermal stress related defects in the growing crystal can be reduced by decreasing the encapsulant thickness to the minimum value compatible with inhibition of arsenic loss from the melt. This finding is in complete disagreement with experimental evidence which indicates that reduction of encapsulant thickness in conventional growth furnaces leads to significant increases in the density of dislocations in the grown solid [1].

NOMENCLATURE

c	specific heat capacity
$\mathrm{d}A$	elemental surface area
∂D_i	boundary i
E	Young's modulus
$F_{\mathrm{d}A_i-\mathrm{d}A_j}$	geometric view factor between surface elements $\mathrm{d}A_i-\mathrm{d}A_j$
$\mathbf{g}$	gravitational vector
k	thermal conductivity
P	pressure
q''	heat flux per unit area
$\bar{q}''$	$q''r_c/k_cT_f$
R	crystal pull rate
Rn	radiation number, equations (9) and (14)
r	radial direction
$\bar{r}$	r/r_c
T	temperature
T_f	solidification temperature of GaAs
u	radial displacement
$\mathbf{V}$	velocity vector
w	axial displacement
z	axial direction
$\bar{z}$	z/r_c
z_e	encapsulant thickness.

Greek symbols

ε	surface emissivity
θ	T/T_f
θ^*	radiative sink temperature
ν	kinematic viscosity
ρ	density
σ	stress
σ_{rs}	resolved shear stress
σ_e	excess stress
σ^*	Stefan–Boltzmann constant
τ	shear stress
ϕ	azimuthal direction.

Subscripts

c	crystal
conv	convection
$\mathrm{d}A_i$	area element on the ith surface
e	encapsulant
F	furnace
i	surface number, $i = 1, 8$
O	opaque encapsulant
rad	radiative
T	transparent encapsulant.

Superscripts

$\bar{}$	non-dimensional quantity.

This study is concerned with a theoretical analysis of the effects of natural convection in the liquid encapsulant on thermal stresses during low pressure LEC (LP-LEC) growth. The influence of variations in the thickness of thermally transparent and opaque encapsulants on convective and radiative heat transfer from the crystal is investigated for two different encapsulant thicknesses as well as total encapsulation of the crystal. The selection of growth conditions in this analysis is aimed at demonstrating a meaningful range of stress profiles as well as identifying the potential of corrective approaches.

THERMAL ANALYSIS

Analysis of heat transfer in the GaAs crystal during LEC growth is based on the geometric model of Fig. 1. The crystal is modelled as a vertical cylinder with a uniform radius of 76 mm (3 in) and a length to radius ratio of 4.0. The crystal top and bottom are modelled as planar surfaces and, thus, do not include the effects of cone-shoulder geometry and the growth interface morphology. The encapsulant/melt interface is assumed to be planar and the crucible wall to extend to the surface of the encapsulant only.

The modes of heat transfer from the crystal surface are radiative exchange to the environment and convective exchange with the gas and the encapsulant. During low pressure LEC growth of GaAs, the convective losses to the ambient gas (usually helium or argon) is negligible compared to radiative interactions [10], and is not considered in this work. During growth the temperature distribution in the solid is

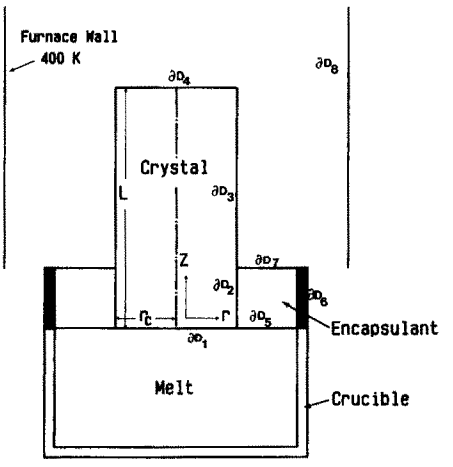

FIG. 1. Geometric model of the crystal, liquid encapsulant, and the growth environment (the melt and part of the crucible containing the melt are not incorporated in the model).

given by

$$\nabla(k\nabla T)+\rho_s c_s R\frac{\partial T}{\partial z}=0 \quad (1)$$

where R is the pull rate. For typical values of growth rate (1–2 cm h^{-1}) the convective effects are negligible ($Pe \sim 0.1$) and the temperature distribution in the solid is well approximated by the solution to the Fourier equation, $\nabla(k\nabla\theta)=0$, where θ is the non-dimensional temperature variable T/T_f.

The temperature and flow field distribution in the encapsulant are obtained by the simultaneous solution of the continuity, Navier–Stokes, and energy equations

$$\nabla\cdot\mathbf{V}=0 \quad (2)$$

$$(\mathbf{V}\cdot\nabla)\mathbf{V}=-\frac{1}{\rho}\nabla P+\nu\nabla^2\mathbf{V}+\mathbf{g} \quad (3)$$

$$(\mathbf{V}\cdot\nabla)T=\alpha\nabla^2 T \quad (4)$$

$$\rho=\rho(T). \quad (5)$$

BOUNDARY CONDITIONS

Velocity field

No slip conditions are imposed at the boundaries of the encapsulant with the crystal and the crucible, ∂D_2 and ∂D_6 of Fig. 1, respectively. As the viscosity of boric oxide significantly exceeds that of the semiconductor melt and the ambient gas the encapsulant/gas and encapsulant/melt boundaries, ∂D_5 and ∂D_7 of Fig. 1, are shear-free surfaces.

Thermal boundary conditions

The thermal boundary conditions are quantified consistent with actual growth conditions and are categorized into temperature and heat-flux conditions.

Temperature boundary conditions. The crystal/melt interface (∂D_1 in Fig. 1) is at the freezing point temperature, T_f ($\theta=1$). The temperature of the melt/encapsulant interface, ∂D_5, is taken to rise linearly from T_f at the crystal edge to 1600 K ($\theta=1.07$) at the crucible wall. In configurations where the encapsulant aspect ratio (ratio of encapsulant height to the crystal radius) is 1 or 1/3, the crucible wall, ∂D_6, is assumed to be uniformly at 1600 K ($\theta=1.07$). In total liquid encapsulation the crucible wall temperature is taken to decrease linearly from 1600 K ($\theta=1.07$) at the melt/encapsulant/crucible contact line to 800 K ($\theta=0.53$), 100 K higher than the glass transformation temperature of boric oxide, at the top of the crucible.

Heat-flux boundary conditions. These conditions are influenced by the transmission of radiant energy through the liquid encapsulant and are formulated for the limiting cases of thermally opaque and transparent encapsulants.

Thermally transparent encapsulant. As a thermally transparent medium, the encapsulant does not interfere with the radiative exchange between the crystal, the melt, the crucible, and the furnace walls. The heat flux at the crystal/encapsulant boundary (∂D_2) is equal to the sum of radiant heat transfer to the environment and convective heat exchange with the liquid encapsulant

$$\overline{q_c''}=\overline{q_{rad}''}+\overline{q_{conv}''} \quad \text{at } \partial D_2. \quad (6)$$

The non-encapsulated portion of the crystal and its top exchange radiant energy with the environment

$$\overline{q_c''}=\overline{q_{rad}''} \quad \text{at } \partial D_3 \text{ and } \partial D_4. \quad (7)$$

The radiative heat transfer at the crystal surface is controlled by the geometric configuration, emissivity and temperature distribution of the surrounding surfaces. By excluding reflection of radiant energy at all surfaces other than that of the crystal, a crystal surface element at some axial location z radiates to an effective radiative sink temperature (RST), θ^*, which is a weighed average of the temperature of all interacting surface elements

$$\overline{q_{rad}''}=Rn_c(\theta_c^4-\theta_{T,2,3}^{*4}) \quad \text{at } \partial D_2 \text{ and } \partial D_3 \quad (8)$$

where

$$Rn_c=\text{crystal radiation number}=\frac{\varepsilon_c\sigma^* T_f^3 r_e}{k_c}. \quad (9)$$

The RST associated with surface elements dA_2 and dA_3 ($\theta_{T,2,3}^*$) is the weighed average of the temperature distribution on surfaces ∂D_5, ∂D_6, and ∂D_8, where the weight coefficients are the geometric view factors from the crystal elements to the elements of these surfaces

$$\theta_{T,2,3}^{*4}(\bar{z})=\sum_{dA_5}F_{dA_{2,3}-dA_5}\theta_{dA_5}^4+\sum_{dA_6}F_{dA_{2,3}-dA_6}\theta_{dA_6}^4+\sum_{dA_8}F_{dA_{2,3}-dA_8}\theta_{dA_8}^4. \quad (10)$$

The crystal top radiates to the furnace walls only, $\theta_{T,4}^*=\theta_F^*$, and as the encapsulant is transparent to thermal radiation, its free surface is an adiabatic boundary.

Thermally opaque encapsulant. Thermal radiation emanating from surfaces in contact with an opaque encapsulant is absorbed within a short distance. Therefore, radiative interaction is inhibited at the encapsulated portion of the crystal and the heat flux at this surface consists only of convective exchange with the encapsulant. The non-encapsulated surface of the crystal (∂D_3) exchanges radiant energy with the free surface of the encapsulant (∂D_7) and the furnace wall (∂D_8)

$$\overline{q_c''}=Rn_c(\theta_c^4-\theta_{O,3}^{*4}) \quad \text{at } \partial D_3 \quad (11)$$

where $\theta_{O,3}^*$ is given by

$$\theta_{O,3}^{*4}=\sum_{dA_7}F_{dA_3-dA_7}\theta_{dA_7}^4+\sum_{dA_8}F_{dA_3-dA_8}\theta_{dA_8}^4. \quad (12)$$

In contrast to the case of a transparent encapsulant, the free surface of an opaque encapsulant radiates to

the crystal and the furnace walls

$$\overline{q''_e} = Rn_e(\theta_7^4 - \theta_{O,7}^{*4}) \quad \text{at } \partial D_7 \tag{13}$$

where

$$Rn_c = \text{encapsulant radiation number} = \frac{\sigma^* T_f^3 r_c}{k_c} \tag{14}$$

and

$$\theta_{O,7}^{*4} = \sum_{dA_3} F_{dA_7-dA_3}\varepsilon_3\theta_{dA_3}^4 + \sum_{dA_8} F_{dA_7-dA_8}\theta_{dA_8}^4. \tag{15}$$

The RST distributions $\theta_{O,3}^*$ and $\theta_{O,7}^*$ are functions of the temperature distribution on the encapsulant free surface and the exposed portion of the crystal, respectively, and are, thus, coupled with the solution of the energy equation in the solid and the encapsulant. Evaluation of $\theta_{O,3}^*$ and $\theta_{O,7}^*$ is discussed in the section on Method of Solution of Equations.

STRESS ANALYSIS

The thermal stress field associated with the calculated temperature distribution is obtained by the solution of thermoelastic equations subject to the condition of traction-free surfaces [10]. Plastic deformation and generation of dislocations in GaAs is associated with crystallographic glide in the $\{111\}\langle 1\bar{1}0\rangle$ slip system, which has twelve possible glide operations. The resolved shear stress for a specified slip plane and direction is obtained by transforming the thermal stress tensor from cylindrical coordinates to the appropriate slip coordinate system. A complete methodology for this transformation and the relationship between the resolved shear stress and the thermal stress components σ_r, σ_ϕ, σ_z and τ_{rz} for the twelve glide operations associated with the $\langle 100\rangle$ growth direction is given in ref. [10]. In the azimuthal direction the resolved shear stress distribution possesses a fourfold symmetry with the maximum values occurring at $\phi = 0$, $\pi/2$, π, and $3\pi/2$ [5]. In this work resolved stresses are calculated along the $\langle 010\rangle$ direction ($\phi = 0$).

As the resolved shear stress, σ_{rs}^i, in any one of the twelve permissible glide operations exceeds CRSS, the crystal undergoes plastic deformation. The extent of plastic deformation in a slip operation is a function of the temperature–thermal stress history experienced by the crystal. However, as a diagnostic indicator we consider, as suggested in ref. [4], the magnitude of plastic deformation to be proportional to the excess of the resolved shear stress over CRSS

$$\begin{aligned} \sigma_e^i &= |\sigma_{rs}^i| - \text{CRSS} \quad |\sigma_{rs}^i| > \text{CRSS} \quad i = 1, 12 \\ \sigma_e^i &= 0 \qquad\qquad\quad |\sigma_{rs}^i| \leqslant \text{CRSS} \quad i = 1, 12. \end{aligned} \tag{16}$$

The total local plastic deformation is, thus, taken to be proportional to the sum of the excess stresses in all glide operations

$$\sigma_e(\bar{r}, \bar{z}) = \sum_{i=1}^{12} \sigma_e^i(\bar{r}, \bar{z}). \tag{17}$$

In studying the effect of different growth parameters on the distribution of excess stress in the crystal, the excess stress is normalized with respect to the local value of the effective CRSS, where the effective CRSS is defined as the product of the number of glide operations and CRSS evaluated at the local temperature

$$\bar{\sigma}_e = \frac{\sigma_e(\bar{r}, \bar{z})}{12^* \text{CRSS}[T(r, z)]}. \tag{18}$$

METHOD OF SOLUTION OF EQUATIONS

The temperature and velocity field in the encapsulant, and the temperature and thermal stress distributions in the crystal are obtained numerically using commercially available codes (natural convection in the encapsulant is solved using FLUENT and the temperature and thermal stress distributions in the solid are obtained using ABAQUS). The geometric view factors, needed for evaluation of the RST distributions, are calculated for discrete surface elements of the interacting planes. For each case study the temperature distribution in the solid, encapsulant, and the RST distributions (for configurations with an opaque encapsulant) are calculated iteratively until a convergant solution is obtained. The energy equations in the encapsulant and the solid are matched by imposing equality of temperature and heat flux at the crystal/encapsulant boundary. On the free surface of the opaque encapsulant (Cases II.1–II.3) linearized radiative boundary conditions, and at the crystal surface non-linear boundary conditions, equations (8), (11) and (13), are used.

The numerical values of the thermophysical properties and model parameters used in the calculations are given in Table 1.

Table 1. Listing of thermoelastic and growth parameters

GaAs [5]	
Thermal conductivity (W cm^{-1} K^{-1})	$2.08T^{-1.09}$
Surface emissivity	0.5
Coefficient of thermal expansion (K^{-1})	$4.88\times10^{-6}+3.82\times10^{-9}T$
Isotropic thermoelastic constant ($\alpha E/(1-\nu)$) (dyn cm^{-2} K^{-1})	$10^{(5.53-557/T)}$
CRSS (dyn cm^{-2} K^{-1})	$10^{(5.83+1382/T)}$
Encapsulant (boric oxide) [5]	
Thermal conductivity (W cm^{-1} K^{-1})	$2.37\times10^{-3}+1.1\times10^{-5}T$
Growth system	
Furnace wall temperature	400 K
Crystal radiation number, Rn_c	0.5
Encapsulant radiation number, Rn_e	1.0

RESULTS

I. *Thermally transparent encapsulant*

I.1. *Aspect ratio* = 1/3. This geometry emulates the most frequently used growth configuration in which the encapsulant thickness is maintained at about 1 cm. The associated axial distribution of heat flux at the crystal periphery as well as its convective and radiative components at the encapsulated portion of the growing solid are presented in Fig. 2. In this figure positive values of q_c'' correspond to heat flux out of and negative values correspond to heat flux into the crystal. The results indicate that the immersed portion of the crystal is radiatively cooled by the environment, whereas convection in the encapsulant promotes heat transfer to the crystal from the crucible and melt. The counteracting influence of radiative and convective heat transfer at the encapsulated portion of the crystal leads to a strong variation in the magnitude and direction of $\overline{q_c''}$. However, radiative losses dominate convective heating effects resulting in an overall positive heat transfer from the immersed portion of the growing solid with the maximum cooling occurring at $\bar{z} \sim 1.5$. The observed positive heat transfer at the crystal surface close to the solidification interface suggests that due to the thermal coupling between the solid and the melt the growth interface morphology will be concave and the assumed planar growth interface will not be sustained during growth.

In the radial direction the crystal undergoes a transition from a state of compression at the core to tension at the periphery. Accordingly, the resolved shear stress exhibits a 'W' shaped profile (i.e. decreasing from the centerline to a minimum at about $\bar{r} \sim 0.5$ and then increasing to its maximum value at the crystal periphery) [4, 10]. As the intent of this study is to investigate the effect of different growth configurations on maximum stresses in the crystal the axial distribution of $\bar{\sigma}_e$ is presented at $\bar{r} = 1$ (Fig. 3). Axially the maximum stresses occur at $\bar{z} \sim 0.75$. The occurrence of maximum stresses at $\bar{z} \sim 0.75$, different from the location of maximum heat fluxes at $\bar{z} \sim 1.5$, reveals the temperature dependence of CRSS and indicates that the location of maximum excess stresses is controlled, in addition to the magnitude of $\overline{q_c''}$ by the local values of CRSS (temperature of the growing solid). The stresses in the crystal are found to exceed CRSS significantly, thus indicating strong driving forces for generation of dislocations.

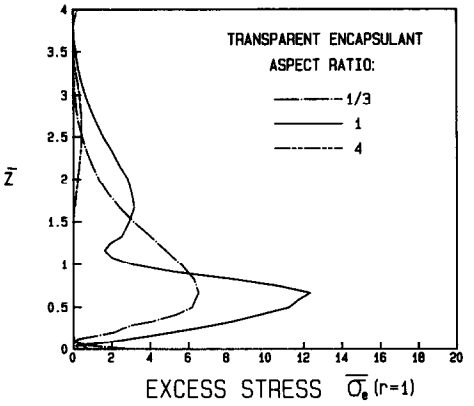

FIG. 3. Axial variation of total excess shear stress ($\bar{\sigma}_e$) at the periphery of GaAs crystals grown with a thermally transparent encapsulant.

I.2. *Aspect ratio* = 1. The axial distribution of heat flux at the crystal periphery and its convective and radiative components are shown in Fig. 4. The calculations indicate that the increase in the crucible wall height (in this work equal to the encapsulant thickness) results in radiative heating of the crystal by the environment as well as enhanced convective

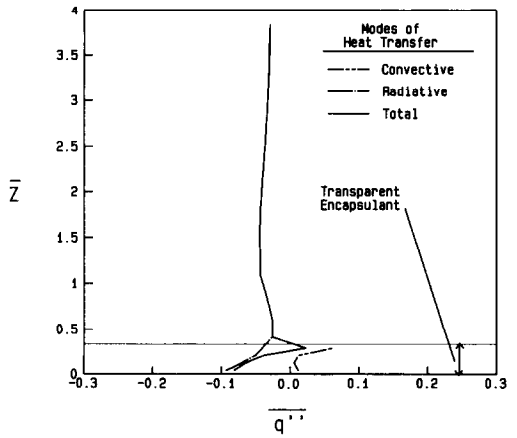

FIG. 2. Axial variation of heat flux at the crystal periphery for a thermally transparent encapsulant corresponding to Case I.1. Negative values of q'' indicate heat transfer out of the crystal surface.

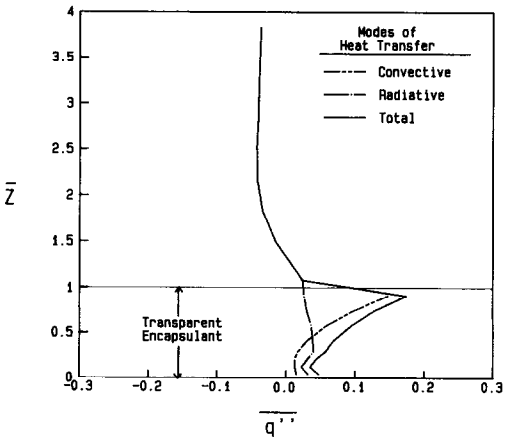

FIG. 4. Axial variation of heat flux at the crystal periphery for a thermally transparent encapsulant corresponding to Case I.2.

exchange with the crucible wall and the melt. Under these conditions the growth interface morphology is expected to be convex into the melt. In the axial direction, as the view factor between the crystal and the furnace walls increases, the heat flux distribution changes sign and beyond $\bar{z} \sim 1.25$ the crystal is radiatively cooled by the environment.

The axial distribution of $\bar{\sigma}_e$ ($\bar{r} = 1$) for this growth configuration (Fig. 3) exhibits a double maximum behavior: the lower peak corresponds to excessive radiative and convective heating of the crystal and the upper peak corresponds to excessive radiative cooling of the solid. As the magnitude of heat input into the lower portion of the crystal is larger than the heat losses toward its top (region of lower local values of temperature and higher values of CRSS), the excess stresses in the encapsulated portion of the crystal are observed to exceed those at the crystal's upper portion by a factor of 6.

The results, thus, indicate that during growth with a transparent encapsulant excessive heating of the lower portion of the crystal is potentially more damaging than cooling of the upper portion of the solid.

I.3. *Aspect ratio* = 4 (*total encapsulation*). The calculated axial heat flux distribution associated with growth at total liquid encapsulation, Fig. 5, indicates that radiative heating of the crystal is offset by convection in the encapsulant which results in overall diminished values of heat flux at the crystal surface. The associated distribution of $\bar{\sigma}_e$ (Fig. 3) exhibits a double-maximum behavior, similar to the previous case, corresponding to heating of the lower portion of the crystal and cooling of its upper portion. However, the stresses are found to be significantly reduced from the previous cases, indicating that growth with total encapsulation of the crystal by a transparent encapsulant and control of the temperature distribution of the crucible wall offers significant potential for reduction of stresses in LEC grown GaAs crystals.

II. *Thermally opaque encapsulant*

II.1. *Aspect ratio* = 1/3. The heat flux distribution at the crystal periphery for this case is presented in Fig. 6. The heat flux distribution at the immersed portion of the crystal represents convective cooling of the crystal by the encapsulant, and the heat losses at its non-encapsulated portion are due to the radiative exchange of the solid with the furnace walls and the encapsulant free surface. The results indicate that radiative losses at the encapsulant top and exposed portion of the crystal, in addition to the relatively low values of thermal conductivity of the encapsulant (about one-fourth that of GaAs), leads to the concentration of cooling effects at the crystal surface in the region close to its point of emergence from the encapsulant. The axial distribution of $\bar{\sigma}_e$ ($\bar{r} = 1$) indicates an associated generation of very large excessive stresses in that region which exceed CRSS by more than one order of magnitude (Fig. 7) and thus imply significant potential for generation of dislocations.

II.2. *Aspect ratio* = 1. Increased thickness of the liquid encapsulant results in the relative thermal isolation of the lower portion of the crystal (Fig. 8). However, similar to the previous case, the crystal experiences significant cooling as it emerges from the encapsulant. The large cooling effects occur at locations more removed from the solidification interface than the previous case (lower values of temperature and higher values of CRSS) and, accordingly, the resulting levels of excess stress are appreciably lowered (Fig. 7). The results, therefore, suggest that increasing the encapsulant thickness can be a significant factor in reduction of stress levels in GaAs crystals grown with an opaque encapsulant.

II.3. *Aspect ratio* = 4 (*total encapsulation*). In this

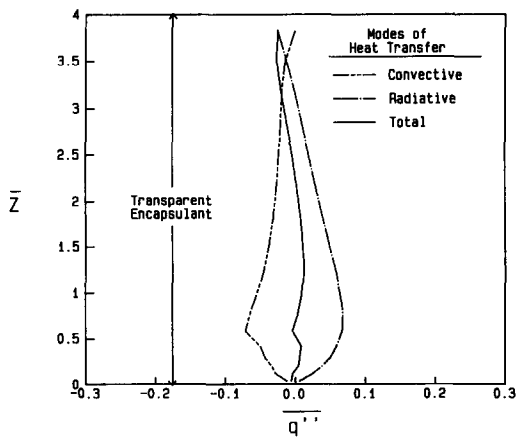

FIG. 5. Axial variation of heat flux at the crystal periphery for a thermally transparent encapsulant corresponding to Case I.3.

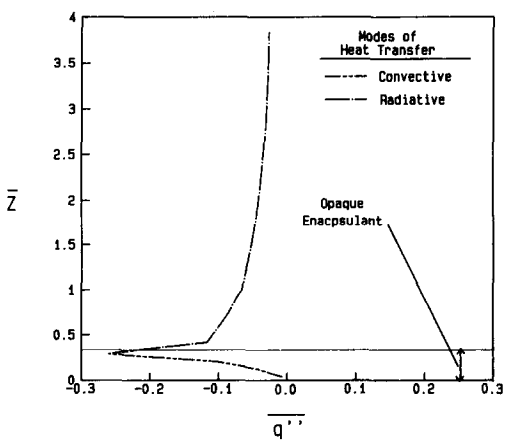

FIG. 6. Axial variation of heat flux at the crystal periphery for a thermally opaque encapsulant corresponding to Case II.1.

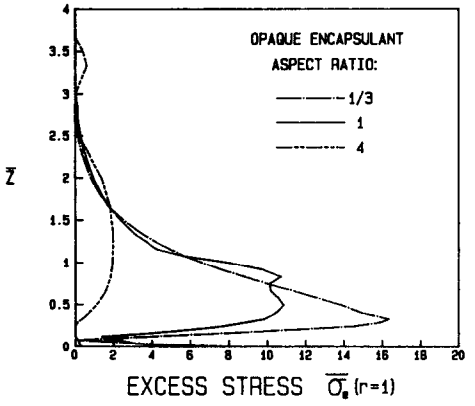

FIG. 7. Axial variation of total excess shear stress ($\bar{\sigma}_e$) at the periphery of GaAs crystals grown with a thermally opaque encapsulant.

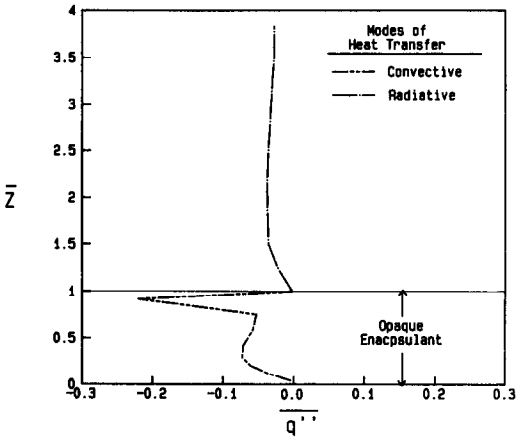

FIG. 8. Axial variation of heat flux at the crystal periphery for a thermally opaque encapsulant corresponding to Case II.2.

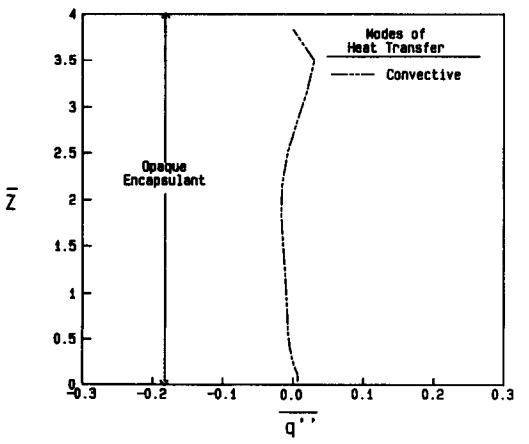

FIG. 9. Axial variation of heat flux at the crystal periphery for a thermally opaque encapsulant corresponding to Case II.3.

configuration, heat loss from the crystal surface is controlled by convective exchange with the encapsulant and the point of emergence of the crystal from the encapsulant is removed to the top of the crystal where the solid's temperature is low, and the local values of CRSS are high. The heat flux distribution is calculated to be significantly lower than the two previous cases (Fig. 9).

The excess stress distribution indicates near elimination of thermal stresses above the plasticity limit in the growing crystal (Fig. 7); and similar to growth with a transparent encapsulant, points to the potential for reduction of stress-related defects in GaAs crystals through total liquid encapsulation of the growing solid.

DISCUSSION

The present thermoelastic analysis of GaAs in a conventional LEC growth configuration indicates that the magnitude of stresses experienced by the crystal exceed CRSS significantly. Variations in the thermal transparency and thickness of the liquid encapsulant influence the magnitude and axial location of maximum excess stresses in the crystal; yet they appear to be inadequate for reduction of stresses to below CRSS. Total encapsulation of the crystal, however, results in virtual elimination of excess stresses for both thermal transparency limits of the encapsulant.

Natural convection in thermally transparent encapsulants at thicknesses of 1/3 to 1 crystal radius promotes heat transfer from the crucible and the melt to the crystal. As the heat transfer from the free surface of a thermally transparent encapsulant to the ambient gas is absent and the temperature of the melt and crucible wall are higher than the freezing point of the crystal, convection in the encapsulant results in heat transfer into the crystal. For the growth configuration with an encapsulant aspect ratio of 1/3, this phenomenon counteracts the radiative losses from the crystal and reduces the heat transfer from the encapsulated portion of the crystal surface. However, with an encapsulant aspect ratio of 1, the convective heating of the crystal is superimposed onto the radiative heat input to the crystal and leads to excessive heating of the solid and an associated generation of maximum stresses in its encapsulated portion. The counteracting influences of convective and radiative effects in the total encapsulation configuration results in a significant overall reduction of heat transfer from the crystal and maximum stresses. Reduction of stress levels to below CRSS for all aspect ratios of the encapsulant requires dynamic control of the temperature of the crucible wall by, e.g. adjusting the location of the continuously decreasing melt level in the hot zone, and control of the furnace wall temperature. The possible occurrence of positive radial temperature gradients in the solid suggests caution in exclusive use of coaxial heat reflectors or after-heaters for increasing the environmental temperature.

For thermally opaque encapsulants, radiative interaction at the encapsulated portion of the crystal is inhibited and maximum heat losses (and the associated maximum excess stresses) occur as the crystal emerges from the encapsulant. Therefore, by increasing the encapsulant thickness, the radiative losses from the encapsulant free surface and the emerging portion of the crystal are reduced (due to lower surface temperatures) and the lower portion of the crystal is thermally isolated from the environment. With the encapsulant thickness equal to 1/3 crystal radius, convective cooling of the crystal does not appear to influence the location and magnitude of maximum excess stresses [10]. Increased encapsulant thickness to 1 crystal radius results in promotion of convective heat losses, and the lower portion of the crystal is significantly cooled with maximum stresses occurring over a large area of the encapsulated portion of the solid. Nevertheless, in spite of enhanced convection in the encapsulant, an increase in the encapsulant aspect ratio from 0.3 to total encapsulation leads to a noticeable reduction in the magnitude of thermal stresses. Control of maximum stress levels to below CRSS requires reduction of heat losses from the crystal during its emergence from the encapsulant, and suggests control of the environment temperature through an appropriate heat transfer control system.

Comparison of the results of this work with a previous study of a similar geometry and thermal boundary conditions but excluding natural convection in the encapsulant [10] indicates that although convection in the encapsulant, for both thermal transparency limits of the encapsulant, influences the magnitude and axial location of the maximum excess stresses in the crystal, it does not significantly alter the trends observed using a conduction dominated solution of the temperature field in the encapsulant. This finding contradicts the assumptions made by Jordan *et al.* [5]. The primary source of the disagreement between Jordan *et al.*'s model and the present results is due to their use of a natural convection correlation valid for vertical bodies in an infinite pool and use of excessively large driving temperature differences in the calculation of the Nusselt number at the crystal/encapsulant interface.

The results of this study suggest that the thermal transparency of the liquid encapsulant strongly controls the magnitude and axial location of maximum stress in GaAs crystals grown by the LP-LEC technique. Recent experimental results on infra-red transmittance of boric oxide [13] indicate that, in the temperature range of interest to melt growth of GaAs, close to 60–70% of the incident energy is absorbed by the encapsulant, and thus, B_2O_3 can be approximated, to the first order, to be opaque to infra-red transmission. Comparison of the modelling results with the experimental data on the axial distribution of dislocations in grown crystals requires, in addition to further investigations into the dynamics and multiplication of dislocations during growth, the extension of the present study to semi-transparent encapsulants and a more detailed modelling of the growth environment.

This study indicates that generation of stress related defects during LEC growth of GaAs can be controlled through the thickness of the encapsulation layer and dynamic adjustment of the 'environmental' temperature. Reduction of thermal stresses during growth is unavoidably associated with a reduction of heat transfer from the crystal and an associated increase in the crystal surface temperature and decreased axial temperature gradients. Thus the time–temperature integral of all parts of the crystal is increased and point defect interaction and clustering are enhanced. Furthermore, reduction of axial temperature gradients in the solid increases the potential for interface breakdown by constitutional supercooling of the melt and, thus, impedes attempts to increase CRSS through solid solution hardening of the matrix by isoelectronic doping. These considerations indicate that identification of specific device-related materials requirements is a crucial factor in optimization of the growth process.

Acknowledgements—The author wishes to express his appreciation for the support provided by DARPA and AFWAL/MLPO (contract No. F33615-83-C-5089) to this project. The continued support of Professor A. F. Witt is also gratefully acknowledged.

REFERENCES

1. C. G. Kirkpatrick, R. T. Chen, D. E. Holmes, P. M. Asbeck, K. R. Elliot, R. D. Fairman and J. R. Oliver, High purity LEC growth and direct implantation of GaAs for monolithic microwave circuits. In *Semiconductor and Semimetals* (Edited by R. K. Willardson and A. C. Beer), Vol. 20, Chap. 1. Academic Press, Florida (1984).
2. P. Petroff and R. L. Hartman, Defect structure introduced during operation of heterojunction GaAs laser, *Appl. Phys. Lett.* **23,** 469–471 (1973).
3. C. Uemura, S. Shinoyama, A. Yamamato and S. Tohno, LEC growth and characterization of undoped InP crystals, *J. Crystal Growth* **52,** 591–596 (1981).
4. A. S. Jordan, A. R. Von Neida and R. Caruso, The theory and practice of dislocation reduction in GaAs and InP, *J. Crystal Growth* **70,** 555–572 (1984).
5. A. S. Jordan, R. Caruso and A. R. Von Neida, A thermoelastic analysis of dislocation generation in pulled GaAs crystals, *Bell Syst. Tech. J.* **62,** 593–677 (1980).
6. P. Penning, Generation of imperfections in germanium crystals by thermal strain, *Philips Res. Rep.* **13,** 79–97 (1958).
7. N. A. Advonin, S. S. Vakhrameev, M. G. Mil'vidskii, V. B. Osvenskii, B. A. Sakharov, V. A. Smirnov and Yu F. Shchelkin, Influence of the temperature field and the thermal stress field upon the formation of the dislocation structure in gallium-arsenide crystals grown by the Czochralski method, *Soviet Phys. Dokl.* **16,** 772–775 (1972).
8. J. C. Brice, The cracking of Czochralski-grown crystals, *J. Crystal Growth* **42,** 427–430 (1977).
9. N. Kobayashi and T. Iwaki, A thermoelastic analysis of the thermal stress produced in a semi-infinite cylindrical single crystal during the Czochralski growth, *J. Crystal Growth* **73,** 96–110 (1985).

10. S. Motakef and A. F. Witt, Thermoelastic analysis of GaAs in LEC growth configuration, Part I: effect of liquid encapsulation on thermal stresses, *J. Crystal Growth* **80**, 37–50 (1987).
11. B. A. Boley and J. H. Weiner, *Theory of Thermal Stresses*, p. 257. Wiley, New York (1960).
12. R. N. Thomas, H. M. Hobgood, G. W. Eldridge, D. L. Barrett, T. T. Braggins, L. B. Ta and S. K. Wang, LEC GaAs for integrated circuit applications. In *Semiconductor and Semimetals* (Edited by R. K. Willardson and A. C. Beer), Vol. 20, Chap. 3. Academic Press, Florida (1984).
13. A. G. Ostrogorsky, K. H. Yao and A. F. Witt, Infrared absorbance of B_2O_3 at temperatures to 1250°C, *J. Crystal Growth* (1987), in press.

EFFET DE LA CONVECTION NATURELLE ET DE LA TRANSPARENCE THERMIQUE DE L'ENCAPSULANT LIQUIDE SUR LES CONTRAINTES THERMIQUES PENDANT LA CROISSANCE LEC DE GaAs

Résumé—On étudie numériquement les effets de la convection naturelle et de la transparence thermique de l'encapsulant liquide sur les distributions de la température et la contrainte élastique dans la croissance des cristaux de GaAs par la technique de Czochralski avec liquide basse pression (LP-LEC). Les résultats montrent que les contraintes dépassent sensiblement CRSS pendant la croissance conventionnelle LP-LEC et qu'elles peuvent être réduites nettement par l'encapsulage total du solide en croissance.

EINFLUSS DER NATÜRLICHEN KONVEKTION UND THERMISCHEN DURCHLÄSSIGKEIT EINES FLÜSSIGKEITSEINSCHLUSSES AUF DIE THERMISCHEN SPANNUNGEN WÄHREND DES LEC-WACHSTUMS VON GaAs-KRISTALLEN

Zusammenfassung—Die Einflüsse natürlicher Konvektion und thermischer Durchlässigkeit eines Flüssigkeitseinschlusses auf die Temperatur- und Spannungsverteilungen in einem GaAs-Kristall—gezüchtet nach dem LP-LEC-Verfahren nach Czochralski—werden numerisch untersucht. Die Ergebnisse zeigen, daß die Spannungen bei normalem LP-LEC-Wachstum CRSS merklich übersteigen und durch totale Einkapselung des wachsenden Feststoffes erheblich eingeschränkt werden können.

ВЛИЯНИЕ ЕСТЕСТВЕННОЙ КОНВЕКЦИИ И ТЕПЛОВОЙ ПРОЗРАЧНОСТИ КАПСУЛЫ С ЖИДКОСТЬЮ НА ТЕПЛОВЫЕ НАПРЯЖЕНИЯ В КРИСТАЛЛАХ GaAs, ВЫРАЩИВАЕМЫХ ПО МЕТОДУ ЧОХРАЛЬСКОГО

Аннотация—Численно изучалось влияние естественной конвекции и тепловой прозрачности капсулы с жидкостью на распределение температуры и упругих напряжений в кристаллах GaAs, выращенных по методу Чохральского при низком давлении. Результаты показывают, что при использовании традиционной методики напряжения значительно превышают сдвиговые напряжения кристаллов и могут быть заметно уменьшены путём капсулирования растущей твёрдой фазы.